

Effect of Concentration upon the Hydrolysis Rate of Ammonium Pyrophosphate at 25 °C

Joseph W. Williard,* Yong K. Kim, and Jack M. Sullivan

Division of Chemical Development, National Fertilizer Development Center, Tennessee Valley Authority, Muscle Shoals, Alabama 35660

The rate of hydrolysis of ammonium pyrophosphate at 25 °C was determined at pH 4, 5, and 6 for solutions containing P₂O₇ concentrations equivalent to 1.39–12.96 wt % P. Apparent first-order rate constants were determined for each solution. Contrary to previous results with ammonium triphosphate, the effect of concentration upon the apparent first-order specific rate constants for pyrophosphate hydrolysis appears minimal. A general linear equation was developed for calculating the rate constant, k_{ap} , when the pH and the equivalent P concentration are known at 25 °C.

Several studies of the rate of hydrolysis of pyrophosphate are reported in the literature (1–7). One of the factors that affects the rate of hydrolysis of a condensed phosphate is its concentration (8). Previous work (9) has demonstrated that concentration has a significant effect upon the specific rate of triphosphate hydrolysis. The apparent first-order rate constants increase with increasing triphosphate content. In this report the influence of concentration upon the specific rate of pyrophosphate hydrolysis at 25 °C and at pH values of 4, 5, and 6 is described. In this case, the initial pyrophosphate concentration was found to have little influence upon the observed first-order rate constants.

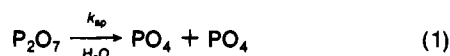
Experimental Section

Three stock solutions were prepared by saturating distilled, deionized water with (NH₄)₃HP₂O₇ (>99%) at pH 4, 5, and 6. Dilution of portions of these stock solutions was made to obtain 77%, 55%, 30%, and 16% of the original solution concentrations. Gaseous ammonia or cation-exchange resin in the H⁺ form was used to adjust the pH of these diluted solutions to the desired value. The diluted solutions, along with portions of the stock solutions, were placed in a water bath at 25 ± 0.2 °C and rotated 4 times/min. The distributions of phosphate species and pH were determined at various times by sampling over a period of 1232 days.

The total phosphorus content of each initial solution was determined gravimetrically (10). The ammoniacal nitrogen content was obtained by basic distillation into standard acid followed by back-titration with NaOH. One-dimensional paper chromatography (11) was used to measure the extent of the pyrophosphate degradation as a function of time. The distribution of pyro- and orthophosphate was determined by cutting the individual bands from the paper and analyzing for P content. A commercial meter with a glass electrode was used to measure pH.

Results and Discussion

Hydrolysis of the pyrophosphate ion proceeds according to the following model:



where P₂O₇ represents the pyrophosphate species and PO₄ represents the orthophosphate species. The hydrolysis of pyrophosphate follows first-order kinetics (12, 13) in the pH range

Table I. Calculated vs. Observed Concentrations of P₂O₇ at 25 °C^a

time, days	pH	P as pyrophosphate, %	
		obsd	calcd
0	6.10	99.3	99.30
1	6.09	98.9	99.26
2	6.07	99.7	99.22
70	6.06	96.9	96.40
71	6.06	97.0	96.36
234	6.08	89.7	89.94
235	6.07	89.9	89.90
364	6.08	85.0	85.12
364	6.08	84.9	85.12
525	6.10	79.3	79.52
525	6.10	79.3	79.52
707	6.08	73.3	73.62
707	6.08	73.3	73.62
954	6.02	66.3	66.32
954	6.03	66.2	66.32
1232	6.09	59.2	58.96
1232	6.09	59.3	58.96

^a Composition: 8.98% N, 12.96% P. N:P₂O₇ ratio: 3.06 mol/mol.

(4–6) and the P concentration range (1–13%) studied. This is shown by the example plots of log (% P as pyrophosphate) vs. time in Figure 1. All the correlation coefficients of the other 14 tests are greater than 0.99, indicating good agreement with the first-order kinetic model.

While the data are fitted well at constant pH by a first-order kinetic model, it is recognized that the mechanism of ammonium pyrophosphate hydrolysis is quite complex. An evaluation of potential mechanisms for the process would require a consideration of the ionization equilibria of pyrophosphoric acid and a determination of the specific reactivity of the individual pyrophosphate ions present in solution (14, 15). It appears that specific hydrogen ion catalysis may play a significant role in this process. However, such an analysis is beyond the scope of the present study.

The apparent first-order rate constants, k_{ap} , for the hydrolysis of P₂O₇ at each pH and P concentration were calculated by regression of the data fitted to the following equation:

$$\log (\% P_2O_7) = a + k_{ap}t/2.303 \quad (2)$$

where log (% P₂O₇) = common logarithm of percent phosphorus present as P₂O₇ at time t (days); a = common logarithm of percent phosphorus present as P₂O₇ at zero time; k_{ap} = first-order rate constant for hydrolysis of P₂O₇ (day⁻¹); t = time (days).

The measured and calculated (eq 2) percentages of phosphorus as pyrophosphate (P₂O₇), along with the nitrogen content of the 12.96% P solution at pH 6, are listed in Table I (the complete table is included in the supplementary material; see paragraph at end of text regarding supplementary material). The calculated rate constants, k_{ap} , are presented in Table II, along with the standard error (SE) of the rate constants and the half-lives for the P₂O₇ species under the indicated conditions. The apparent first-order rate constants are in good agreement

Table II. Calculated Constants of P₂O₅ Concentration Effect on Rate of Hydrolysis of Pyrophosphate at 25 °C

solution no.	composn, %		pH (av)	k_{ap} , day ⁻¹	10 ⁴ [SE(k_{ap})], ^a day ⁻¹	$t_{0.5}$, ^b days
	N	P				
1	4.92	10.20	4.04	0.001 706 6	0.4575	405
2	3.75	7.81	4.13	0.001 753 7	0.1264	396
3	2.71	5.69	4.14	0.001 721 4	0.0844	402
4	1.38	3.01	4.14	0.001 701 8	0.0830	408
5	0.76	1.69	4.12	0.001 697 4	0.1215	408
6	6.17	10.86	4.99	0.001 061 6	0.1523	654
7	4.69	8.41	5.03	0.001 015 5	0.1368	680
8	3.28	6.02	5.06	0.001 019 9	0.1270	680
9	1.67	3.22	5.07	0.001 125 0	0.1274	619
10	0.70	1.39	5.09	0.001 193 5	0.1036	582
11	8.98	12.96	6.08	0.000 423 2	0.0232	1639
12	6.39	10.10	5.75	0.000 607 6	0.0557	1140
13	4.65	7.18	5.97	0.000 441 3	0.0289	1572
14	2.58	4.05	5.97	0.000 450 8	0.0326	1537
15	1.29	2.09	5.99	0.000 503 3	0.0393	1378

^aSE = standard error. ^bHalf-life.

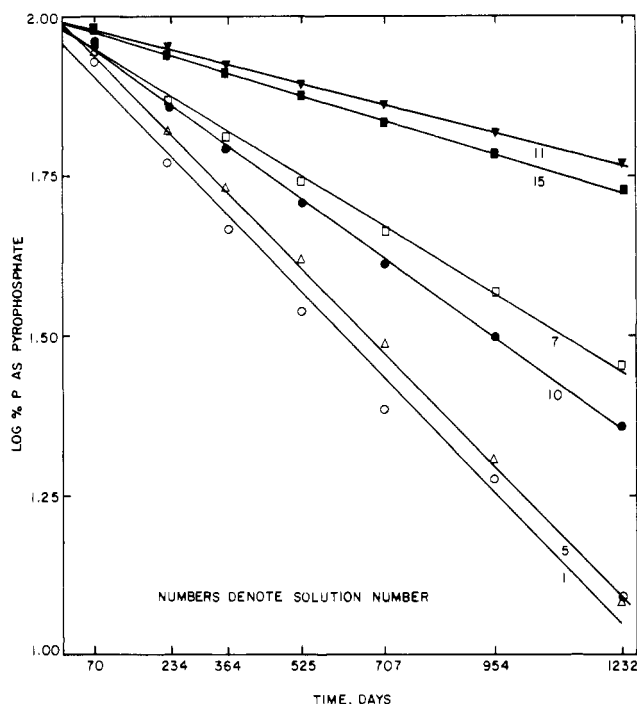


Figure 1. Rate of hydrolysis of ammonium pyrophosphate at 25 °C.

with those obtained previously (9) for the consecutive two-step hydrolysis of ammonium tripolyphosphate.

Figure 2 shows the relationship between concentration and k_{ap} at pH 4, 5, and 6, respectively. Within experimental error, there appears to be little influence of concentration upon the specific rate of pyrophosphate hydrolysis. This result is in contrast with that of the ammonium tripolyphosphate study (9), in which there was an increase in the specific rate of hydrolysis with increase in tripolyphosphate concentration. There are only four points on the curve of pH 6 because there was a misadjustment of the solution pH for the 10.10% P solution (see solution no. 12, supplementary material).

The following general equation was developed to express the influence of pH and any slight effect of P concentration upon the apparent first-order rate constants, k_{ap} , for pyrophosphate hydrolysis at 25 °C:

$$k_{ap} = 0.004570 - 0.00003406C - 0.0006681(\text{pH}) + 0.0000020C^2 \quad (3)$$

where C is the concentration of P₂O₇ expressed as wt % P. Even though the effect of the concentration on the rate con-

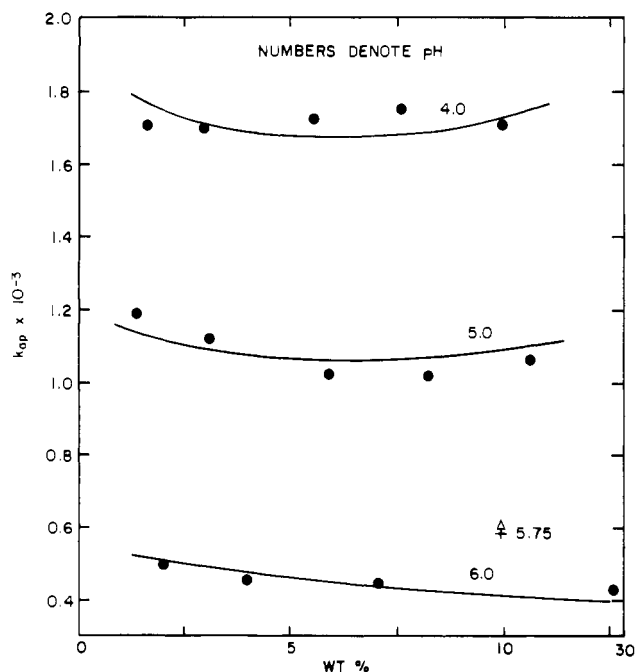


Figure 2. Pyrophosphate hydrolysis rate constants, k_{ap} , affected by P concentration and pH at 25 °C.

stant, k_{ap} , is very small (as indicated by the small coefficient for the C and C^2 terms), the contribution is still statistically significant (95% confidence level). The correlation coefficient is 0.993 and the standard deviation (SD) is 4.3%. The curves in Figure 2 were calculated from eq 3 to show the agreement between calculated and observed k_{ap} values. The plotted points were obtained experimentally. To show the reliability of eq 3, the results of the pH-misadjusted solution 12 (see supplementary material) were plotted showing the experimental k_{ap} as indicated by Δ and the calculated value by $+$. The difference between the experimental results and the predicted value is 3.3%.

Registry No. (NH₄)₂HP₂O₇, 13813-81-5.

Literature Cited

- (1) Strauss, U. P.; Day, J. W. *J. Polym. Sci., Part C* **1967**, *16*, 2161-9.
- (2) Bell, R. N. *Ind. Eng. Chem.* **1947**, *39*, 136-40.
- (3) Bunton, C. A.; Chalmovich, H. *Inorg. Chem.* **1965**, *4*, 1763-8.
- (4) Friess, S. L. *J. Am. Chem. Soc.* **1952**, *74*, 4027-9.
- (5) Crowther, J. P.; Westman, A. E. R. *Can. J. Chem.* **1956**, *34*, 969-81.
- (6) Munson, R. A. *J. Phys. Chem.* **1965**, *69*, 1761-2.
- (7) Campbell, D. O.; Kilpatrick, M. L. *J. Am. Chem. Soc.* **1954**, *76*, 893-901.
- (8) Van Wazer, J. R. "Phosphorus and Its Compounds"; Interscience: New York, 1968; Vol. 1.

- (9) Williard, J. W.; Sullivan, J. M.; Kim, Y. K. *J. Chem. Eng. Data* 1984, 29, 290-3.
- (10) Perrin, C. H. *J. Assoc. Off. Anal. Chem.* 1958, 41, 758-63.
- (11) Karl-Kroupa, E. *Anal. Chem.* 1956, 28, 1091-7.
- (12) Williard, J. W.; Farr, T. D.; Hatfield, J. D. *J. Chem. Eng. Data* 1975, 20, 276-83.
- (13) Van Wazer, J. R.; Griffith, E. J.; McCullough, J. F. *J. Am. Chem. Soc.* 1952, 74, 4977-8.
- (14) Campbell, D. O.; Kilpatrick, M. L. *J. Am. Chem. Soc.* 1954, 76, 893-901.

- (15) Osterheld, R. K. *J. Phys. Chem.* 1958, 62, 1133-5.

Received for review November 21, 1983. Accepted May 21, 1984.

Supplementary Material Available: Complete Table I (calculated vs. observed concentrations of P₂O₇ at 25 °C) (8 pages). Ordering information is given on any current masthead page.

Vapor-Liquid Equilibrium for 1-Methylnaphthalene/Methanol Mixtures at Elevated Temperatures and Pressures

Mark C. Thies and Michael E. Paulaitis*

Department of Chemical Engineering, University of Delaware, Newark, Delaware 19716

Vapor and liquid equilibrium compositions have been measured for binary 1-methylnaphthalene/methanol mixtures at 246.4, 272.2, and 296.9 °C over a range of pressures from approximately 1.3 MPa to the respective mixture critical pressures. Mixture critical pressures are obtained by visual observation of critical opalescence within the view cell.

Introduction

Experimental investigations of fluid-phase equilibria at elevated temperatures and pressures are relatively scarce for mixtures containing model coal compounds with dense fluids, such as water, methanol, or ammonia. Such information is important, however, for the design and evaluation of potential coal conversion processes in general and is of particular interest for potential conversion processes that could utilize these dense fluids as extractive solvents.

In this work, a new flow experimental technique is described for measuring equilibrium compositions, temperatures, and pressures for binary and multicomponent mixtures coexisting in two fluid phases at temperatures up to 450 °C and pressures up to 5000 psi. Measured vapor and liquid equilibrium compositions are reported for binary 1-methylnaphthalene/methanol mixtures at temperatures between approximately 250 and 300 °C, and at pressures up to the mixture critical point. The apparatus includes a view cell for observing phase equilibrium behavior. This visual capability is an important feature for measurements near the critical point and for determining mixture critical temperatures and pressures.

Chao and co-workers (1) have used a similar experimental technique to measure vapor-liquid equilibrium at elevated temperatures and pressures for binary mixtures containing model coal compounds, such as 1-methylnaphthalene, with supercritical gases, such as hydrogen (2), carbon dioxide (3), and methane (4). These investigators have published extensively on work involving several other model coal compounds with each of these supercritical gases and have more recently reported results for binary mixtures containing nitrogen (5), and ternary mixtures containing two supercritical gases (6). Their experimental method does not have viewing capabilities; however, a new flow method has been described which does include a view cell (7).

Wilson and Owens (8) have also reported using a flow technique with a view cell to measure vapor-liquid equilibrium at elevated temperatures and pressures for mixtures of coal

liquids with hydrogen, methane, and hydrogen sulfide.

Experimental Section

A schematic diagram of the apparatus is shown in Figure 1. A flow technique is used to facilitate sampling at elevated pressures and to minimize thermal degradation by reducing residence times for the mixtures at elevated temperatures. Methanol and 1-methylnaphthalene are delivered as compressed liquids by separate high-pressure feed pumps (Milton Roy Model no. 396 Minipumps). The preheater/mixer consists of 0.635 cm i.d. tubing approximately 1 m in length which contains a helical steel ribbon to promote mixing and is wound with electrical tape to heat the mixture to within 1 °C of the desired operating temperature. The total constant flow rate from the two feed pumps ranges from 250 to 500 mL/h. The desired operating temperature is achieved by further heating in 0.076 cm i.d. tubing approximately 1.5 m in length which is located within the constant-temperature bath. The equilibrated, two-phase mixture is then fed to the view cell which functions as a phase separator. The gas or fluid phase of lower density subsequently exits at the top of the cell and is expanded to atmospheric pressure across a micrometering valve (Autoclave Engineers Model no. 30 VRM). The pressure letdown also results in cooling so that a liquid sample is collected. The liquid or fluid phase of higher density exits at the bottom of the cell and is expanded in a similar manner to ambient conditions. Compositions of both samples are determined by analysis with a Hewlett-Packard 5880A gas chromatograph utilizing a flame ionization detector.

The view cell was purchased from Jacoby-Tarbox Corp. and has been modified in our laboratory for operation above 100 °C. The cell consists of a 316 stainless steel enclosure with windows on opposite faces to enable observation along the entire vertical length of the inside of the cell. The cell windows are made of high-temperature aluminosilicate glass (Hoya Corp.) mounted on graphite gaskets with specially designed brass antiextrusion rings. The maximum operating conditions for the cell are limited by the windows and are estimated to be 450 °C at 5000 psi. The internal volume of the cell is approximately 60 cm³.

The thermostat consists of a forced-convection, nitrogen bath sealed from outside air and surrounded by insulation. Vycor windows on opposite sides of the bath permit observation into the view cell. For the safety of the observer, a polycarbonate shield is also mounted over the viewing window. Heating is achieved by circulating the nitrogen across three Chromalox